Applied Ocean Research 32 (2010) 191–208

Contents lists available at ScienceDirect

Applied Ocean Research

journal homepage: www.elsevier.com/locate/apor

Estimating wave spectra from the motions of moored vessels: Experimental validation

Alexandre N. Simos [a,*], Eduardo A. Tannuri [b], João V. Sparano [a], Vinícius L.F. Matos [c]

[a] Naval Arch. & Ocean Eng. Department, Escola Politécnica – University of São Paulo, Brazil
[b] Mechatronics Eng. Department, Escola Politécnica – University of São Paulo, Brazil
[c] Exploration and Production, Petrobras, Brazil

ARTICLE INFO

Article history:
Received 23 April 2009
Received in revised form
7 August 2009
Accepted 10 October 2009
Available online 6 November 2009

Keywords:
Directional wave spectrum
Motion-based estimation
FPSO vessel
Experimental validation

ABSTRACT

The practicability of estimating directional wave spectra based on a vessel's 1st order response has been recently addressed by several researchers. Different alternatives regarding statistical inference methods and possible drawbacks that could arise from their application have been extensively discussed, with an apparent preference for estimations based on Bayesian inference algorithms. Most of the results on this matter, however, rely exclusively on numerical simulations or at best on few and sparse full-scale measurements, comprising a questionable basis for validation purposes. This paper discusses several issues that have recently been debated regarding the advantages of Bayesian inference and different alternatives for its implementation. Among those are the definition of the best set of input motions, the number of parameters required for guaranteeing smoothness of the spectrum in frequency and direction and how to determine their optimum values. These subjects are addressed in the light of an extensive experimental campaign performed with a small-scale model of an FPSO platform (VLCC hull), which was conducted in an ocean basin in Brazil. Tests involved long and short crested seas with variable levels of directional spreading and also bimodal conditions. The calibration spectra measured in the tank by means of an array of wave probes configured the paradigm for estimations. Results showed that a wide range of sea conditions could be estimated with good precision, even those with somewhat low peak periods. Some possible drawbacks that have been pointed out in previous works concerning the viability of employing large vessels for such a task are then refuted. Also, it is shown that a second parameter for smoothing the spectrum in frequency may indeed increase the accuracy in some situations, although the criterion usually proposed for estimating the optimum values (ABIC) demands large computational effort and does not seem adequate for practical on-board systems, which require expeditious estimations.

1. Introduction

Wave spectrum estimation from a vessel's motions is a lively research topic that has recently been addressed by many authors. Interest in the subject comes primarily from the prospect of on-board estimations requiring quite simple instrumentation and hardware, basically involving an ordinary set of accelerometers and rate-gyros connected to a PC. The method could therefore represent an uncomplicated and inexpensive choice for wave inference, if compared to wave buoys and radar systems.

At Escola Politécnica — USP, an extensive research program has been conducted since the year 2000, aiming to evaluate the possibility of estimating wave spectrum on-board offshore systems, like FPSO platforms. This program has been fully supported by Petrobras, which financed a series of ocean basin tests and also provided full-scale data measured on some of their platforms in order to supply a significant basis for the validation of the proposed methodology. On-board estimation of wave spectra in offshore systems may be useful for several reasons. First of all, some floating units may experience operational problems caused by large vertical motions induced by waves. The information about the spectrum can then be used in safety procedures, aiming to reduce the risks of the operation or to keep the integrity of the installations. For example, such information might be used to relocate an FPSO to a safer wave heading, either by using tugboats or dynamic positioning systems. Furthermore, the estimation would be also useful for other types of ships, like crane barges and pipe-laying vessels, since the information can be help its crew to evaluate the feasibility of a particular operation or the need to interrupt it. Other applications that may be envisaged are related to Dynamic Positioning (DP) systems. As offshore oil production moves towards deeper waters, DP systems become increasingly important as an economical solution for

* Corresponding author. Fax: +55 11 30915717.
E-mail address: alesimos@usp.br (A.N. Simos).

0141-1187/$ – see front matter © 2009 Elsevier Ltd. All rights reserved.
doi:10.1016/j.apor.2009.10.004

Nomenclature

ε_{1mk}	second-order difference of spectrum associated to direction k at frequency m
ε_{2mk}	second-order difference of spectrum associated to the frequency m at the direction k
ϕ_{mn}	cross spectra of ship motions "m" and "n"
θ	wave direction $[0; 2\pi]$
σ^2	noise variance
ω	frequency (rad/s)
$\mathbf{A}$	RAO matrix
$\mathbf{B}$	vector with cross spectra of ship motions
$\mathbf{H}_1, \mathbf{H}_2, \mathbf{H}_3$	matrices defined in (8)–(10) used to describe the prior distribution function
H_s	significant wave height
$J(x)$	functional to be minimized in the Bayesian method
K	number of angular intervals used in the discretization
$L(x\|B)$	*likelihood function*
M	number of wave frequencies used in the discretization
N	number of vessel's motions used in the method
$p(x)$	prior distribution function of the spectrum
P	number of integral equations derived from (1)
RAO_m	Response Amplitude Operator (Transfer Function) of ship's motion "m"
$S(\omega, \theta)$	directional wave spectrum
T	hull draft
T_p	peak period
$\mathbf{U}$	vector with measurement noise
u_1, u_2	parameters that controls the trade-off between good fit to the data and smoothness of the spectrum
u_3	parameter that controls the spectrum energy at the frequency boundaries
x	vector with the components of directional wave spectrum

the station-keeping of floating production units and other vessels. For DP operations under extreme conditions, feed-forward control may represent a significant improvement in the efficiency of the system, concerning station-keeping behavior and fuel consumption. The feed forward control consists of providing information on the environmental excitation (waves, current and winds) to the system in order to predict the DP response required for counteracting the estimated environmental forces. On-board estimation of directional wave spectrum may then play an important role on the wave force feed-forward control.

Not so long ago, wave measurements in oil & gas basins offshore from Brazil depended exclusively on moored wave-buoys. Such devices provide good estimates of wave spectra, since they have negligible dynamics and their motions can be accurately measured by means of accelerometers and tilt sensors. However, buoys are easily subjected to damage and loss, and also suffer from practical and economical drawbacks related to deep water mooring. Recently, wave-monitoring radar systems have been developed based on the analysis of temporal and spatial evolution of the radar backscatter information. Such systems may be installed on-board, consequently eliminating the problems associated with moored buoys. On the other hand, they require an extensive calibration campaign and, according to platform personnel, estimations might be influenced by meteorological conditions in the measurement site.

Estimation of wave spectra based on a ship's motions may present an alternative that overcomes such problems and, due to its inherent simplicity, it might even be foreseen as a complement to other methods. Different approaches for this kind of estimation have been studied recently, mainly involving parametric or Bayesian estimation models. In fact, the latest seems to be gaining preference especially for requiring much less computational effort if compared to parametric modeling, which ultimately leads to a nonlinear optimization problem. Indeed, the computational time required by the estimation models is a crucial issue regarding their practical application on-board and may impose limitations to the methods, as will be discussed later.

1.1. Overview of recent works in the field

Regarding the methodology, a brief review of some recent works may provide an overview of the alternatives that have been tested and call attention to the discussion on their possible advantages and drawbacks. As examples of the application of parametric modeling one may find the works of Hua and Palmquist [1] and Tannuri et al. [2], the latter dealing with the problem of a moored vessel (FPSO platform) and developed within the context of the same research project that includes the present paper. The model adopted by Tannuri et al. leads to a nonlinear optimization problem involving 10 parameters and therefore requires extensive computational time. Working with a VLCC, they point out that the ship filters the high-frequency components of the waves (when there is no appreciable 1st order response) and estimates *cut-off* periods associated to this kind of vessel. Obviously, this is a drawback that is shared by all different methods that intend to derive the spectral estimations from ship's motions. The problem was later re-examined by Nielsen [3], although now dealing with a Bayesian estimation. Another problem that was addressed by Tannuri et al. was the sensitivity to errors in the transfer functions of motions (the so-called Response Amplitude Operators — RAOs). Once again, this is a problem common to all the methods, but it is frequently overlooked. When the ship is used as a wave-buoy, it must be recalled that one is interested in estimating wave components within the frequency range where the ship has significant dynamic response, including usual resonances in heave and roll motions. Roll motion is indeed, by far, the most difficult to reproduce appropriately in a linear analysis, since it is often resonant, lowly damped and the damping is dominated by nonlinear (viscous) hydrodynamic effects. As a consequence, linear analysis requires linearization of the damping with respect to a pre-established amplitude of motion. Obviously, these characteristics are quite inappropriate when wave estimation is concerned. As noticed by Tannuri et al., previous works regarding motion-based wave estimations usually adopted the classical set of heave-pitch-roll motions, a clear consequence of the wave-buoy analogy. As an alternative, they show that the roll motion could be easily replaced by the sway motion, which brings the same information regarding wave direction with respect to the hull. By doing this, the reliability on the set of transfer functions is unquestionably increased. Nielsen [4] later revisited this possibility and confronted the results based on the different set of motions with the full-scale data recorded by a radar system operating in a container ship. Although Nielsen concludes that "the analysis did not suggest to use the roll response in favor of the sway response, or vice-versa", the results presented significant variations in estimated wave height and direction when roll or sway was used. Also, by evaluating the results presented in the paper, one realizes that the highest errors in H_S estimated by the Bayesian method (26%) occurred for the situation with the largest wave height (7.2 m) and period (10.1 s), when substitution of the roll motion indeed led to a closer agreement with the radar results. This does not seem to be a coincidence since it might be argued that nonlinear effects in the roll motion increase with wave height and also as the wave period come closer to the roll natural period (usually above 10 s). Moreover, it must be recalled that when FPSO

platforms are concerned, the probability of errors in the roll transfer function is much larger than for conventional ships. First of all, the vessel loading (and draft) is continuously changing and errors in KG and inertia values may lead to wrong estimations of the natural period. Also, the effect of mooring lines and risers on the roll damping is extremely difficult to predict in full-scale.

Iseki and Ohtsu [5] proposed the application of a Bayesian inference procedure to the problem of ship-based wave estimation. Aiming at the problem of ships on the move, they deal with the encounter frequency and direction and the problem that arises in following seas (the well-known triple-valued problem). In the first version of the method, the smoothness of the spectrum with respect to frequency and direction was guaranteed by only one (hyper)parameter. The value of this parameter should be estimated *a posteriori* by a criterion such as the ABIC (Akaike's Bayesian information criterion, [6]). Later, Nielsen [7] showed that problems may arise when applying ABIC to a single hyperparameter and introduced a second one, with favorable results.

Pascoal et al. [8] presented a first comparison between parametric and non-parametric (Bayesian) models, using heave-sway-pitch motions, as previously suggested by Tannuri et al. Authors observed that, although parametric representation leads to inherently smooth estimations, the method presents several disadvantages when compared to the non-parametric model, the most important of which were related to the computational time consumption and the difficult convergence of the numerical algorithm. On the other hand, some problems were also reported when using the non-parametric model, especially shifts of 180° in the estimated directions (according to the authors, a problem already observed by Iseki [9]). The authors correctly argue that the heave response is probably the single most important one. However, the argument is used to conclude that large vessels (such as VLCCs, for example) would be "very poor estimators" since the heave transfer function would have zeros within the wave frequency range with significant energy. Results shown ahead in the present paper shows that this is not the case, as short-crested seas with relatively low peak periods can indeed be well predicted even by a fully loaded VLCC. Further comparisons of Bayesian and parametric model were presented by Nielsen [3,4].

Finally, in the context of the present research project, a preliminary test of Bayesian and parametric estimators with full-scale data was presented by Simos et al. [10], making use of data obtained in a monitoring campaign of an FPSO unit that operates in the Campos Basin. Results were compared with the data provided by a wave-buoy installed in the vicinity of the unit. Unfortunately, due to technical problems experienced by the buoy, data was sparse and restricted to very mild wave conditions. Nonetheless, a few comparisons could be made, which showed that the parametric model failed to provide good estimations in most cases. Bayesian estimation presented better results and, as already observed in previous works, demanded much less computational time.

Apart from the full-scale measurements, an extensive experimental campaign was performed, with a small-scale model of the same FPSO unit in order to extend the data available for evaluation and validation of the estimation models. This campaign is the main subject of the present work, as detailed next.

1.2. The scope of this work

From the discussion above, one may appreciate that a considerable number of works in the field has recently been presented. However, most of the previous analysis is based exclusively on numerical simulations or depends on comparisons with sparse full-scale data, mainly derived from radar systems. In the context of this research project, a series of small-scale tests has been conducted at the LabOceano ocean basin, in Rio de Janeiro, comprising both, long and short-crested seas, the later with variable levels of directional spreading. Combined (swell and wind) seas, a common condition in the Campos Basin, were also tested. A small-scale (1:70) model of the P-35 FPSO unit has been subjected to bow, quartering and beam seas with different wave heights and peak periods.

The Bayesian inference method with two hyperparameters (as proposed by Nielsen [7]) was adopted and the ABIC method for evaluating their optimum values was tested in some cases. Roll was excluded from the input motions, which comprised all the other five motions (including surge and yaw). Wave spectra estimated from the model motions were directly compared to those measured in the basin by means of an array of wave probes. Very good estimations of the statistical parameters (significant wave height, peak period and mean wave direction) were obtained and, in most cases, even the directional spreading could be properly predicted. Inversion of the mean direction (180° shift), mentioned by some authors as a possible drawback of the Bayesian inference method, was not observed in any case. It is shown that some problems related to zeros in the heave transfer function may indeed arise in some situations (as previously argued by Pascoal et al. [8]), but they are localized (confined to a narrow range of frequencies) and do not represent a serious hazard to the predicted statistics. Furthermore, it is demonstrated that this errors may be avoided when the optimum solution can be found by the ABIC method, although with the expense of significant computational effort, which may render it unpractical for real on-board estimations. Sensitivity analysis on errors in the input parameters, such as the vessel inertial characteristics, has also been performed and attested that the method is robust enough to cope well with the expected level of uncertainties.

Next, the statistical model is presented, followed by a description of the experimental setup and the discussion of illustrative results.

2. The Bayesian method

In this section the Bayesian estimation method is briefly presented, focusing on its application to the motion-based wave spectrum estimation. The formulation adopted here follows the one proposed Nielsen [7] closely, using two different hyperparameters in order to control the smoothness in direction and frequency.

Assuming linearity between waves and ship response, the cross-spectra derived from the time series of ship motions (ϕ_{ij}) and the directional wave spectrum are related by the RAOs through the following integral:

$$\phi_{ij}(\omega) = \int_{-\pi}^{\pi} \mathrm{RAO}_i(\omega,\theta)\cdot \mathrm{RAO}_j^*(\omega,\theta)\cdot S(\omega,\theta)\cdot \mathrm{d}\theta, \tag{1}$$

where RAO_i denotes the Response Amplitude Operator of the motion i at frequency ω and direction of incidence θ and $S(\omega,\theta)$ denotes the directional wave spectrum.

The discrete expression of (1) is derived assuming the integrand to be constant on each slice $\Delta\theta = 2\pi/K$:

$$\phi_{ij}(\omega) = \Delta\theta \sum_{k=1}^{K} \mathrm{RAO}_i(\omega,\theta_k)\cdot \mathrm{RAO}_j^*(\omega,\theta_k)\cdot S(\omega,\theta_k), \tag{2}$$

with $\theta_k = -\pi + (k-1)\Delta\theta$.

A certain range of M wave frequencies is specified in advance $(\omega_1, \omega_2, \ldots, \omega_m, \ldots, \omega_M)$ and, being $\Delta\omega = (\omega_M - \omega_1)/(M-1)$, Eq. (2) can be rewritten as:

$$\mathbf{B} = \mathbf{A}\cdot\mathbf{x} + \mathbf{U}. \tag{3}$$

$$\mathbf{A}_m = \begin{bmatrix} |\mathrm{RAO}_i(\omega_m,\theta_1)|^2 & \dots & |\mathrm{RAO}_i(\omega_m,\theta_k)|^2 & \dots & |\mathrm{RAO}_i(\omega_m,\theta_K)|^2 \\ & & \vdots & & \\ \mathrm{Re}\left(\mathrm{RAO}_i(\omega_m,\theta_1)\mathrm{RAO}_j(\omega_m,\theta_1)^*\right) & \dots & \mathrm{Re}\left(\mathrm{RAO}_i(\omega_m,\theta_k)\mathrm{RAO}_j(\omega_m,\theta_k)^*\right) & \dots & \mathrm{Re}\left(\mathrm{RAO}_i(\omega_m,\theta_1)\mathrm{RAO}_j(\omega_m,\theta_K)^*\right) \\ & & \vdots & & \\ \mathrm{Im}\left(\mathrm{RAO}_i(\omega_m,\theta_1)\mathrm{RAO}_j(\omega_m,\theta_1)^*\right) & \dots & \mathrm{Im}\left(\mathrm{RAO}_i(\omega_m,\theta_k)\mathrm{RAO}_j(\omega_m,\theta_k)^*\right) & \dots & \mathrm{Im}\left(\mathrm{RAO}_i(\omega_m,\theta_1)\mathrm{RAO}_j(\omega_m,\theta_K)^*\right) \\ & & \vdots & & \end{bmatrix}$$

Box I.

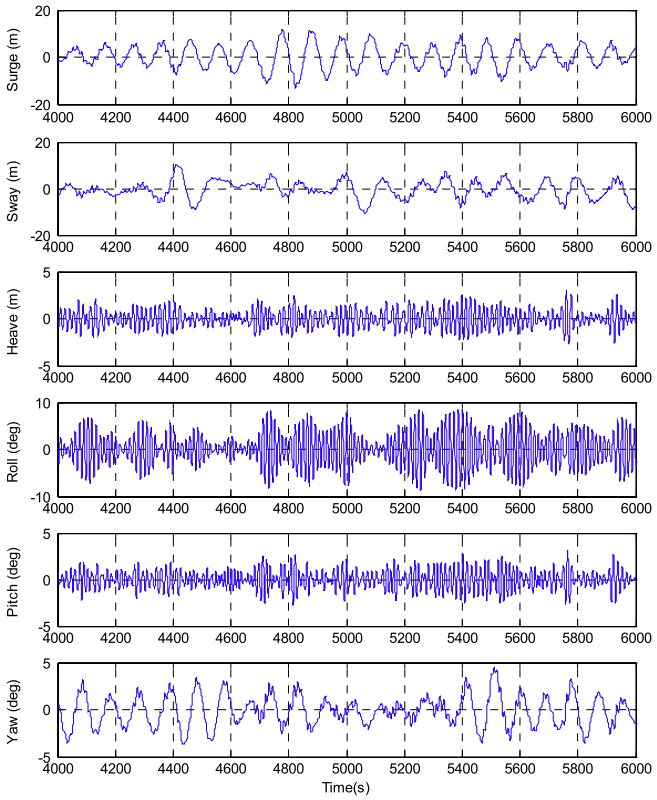

Fig. 1. Example of time series of motion.

The vector $\mathbf{x}$ contains the unknown spectrum evaluated at the $(K \cdot M)$ pairs (ω_m, θ_k):

$$\mathbf{x} = \begin{bmatrix} S(\omega_1,\theta_1) \\ S(\omega_1,\theta_2) \\ \vdots \\ S(\omega_M,\theta_{K-1}) \\ S(\omega_M,\theta_K) \end{bmatrix}.$$

The vector $\mathbf{B}$ contains $(N^2 \cdot M)$ elements related to the spectrum and cross-spectrum of the (N) measured vessel's motions $\phi_{ij}(\omega_m)$ and is given by:

$$\mathbf{B} = [\,\mathbf{b}_1 \quad \mathbf{b}_2 \quad \dots \quad \mathbf{b}_M\,]^T, \quad \text{with } \mathbf{b_m} = \begin{bmatrix} \phi_{ii}(\omega_m) \\ \vdots \\ \mathrm{Re}[\phi_{ij}(\omega_m)] \\ \vdots \\ \mathrm{Im}[\phi_{ij}(\omega_m)] \\ \vdots \end{bmatrix}. \tag{4}$$

$\mathbf{U}$ is a $(N^2 \cdot M)$ vector representing measurement noise, assumed to be a Gaussian white noise sequence with zero mean value and variance σ^2 and $\mathbf{A}$ is the $(N^2 \cdot M) \times (K \cdot M)$ RAO matrix given by:

$$\mathbf{A} = \begin{bmatrix} \mathbf{A_1} & \mathbf{0} & \cdots & \mathbf{0} \\ \mathbf{0} & \mathbf{A_2} & \cdots & \mathbf{0} \\ \vdots & \vdots & \ddots & \\ \mathbf{0} & \mathbf{0} & & \mathbf{A_M} \end{bmatrix} \tag{5}$$

with $\mathbf{0}$ the $N^2 \times K$ matrix with null elements (see Box I).

Applying the Bayesian procedure to the system in Eq. (3), the unknown coefficients (vector $\mathbf{x}$) can be estimated by maximizing the product of the likelihood function by the prior distribution.

The likelihood function is the conditional probability of occurrence of a given measurement (matrix $\mathbf{B}$), given the directional spectrum (vector $\mathbf{x}$). Since measurement noise is assumed to be Gaussian, it can be shown that the likelihood function $L(\mathbf{x}|\mathbf{B})$ is given by:

$$L(\mathbf{x}|\mathbf{B}) = \left(\frac{1}{2\pi\sigma^2}\right)^{N^2/2} \exp\left(-\frac{1}{2\sigma^2}\,\|\mathbf{B}-\mathbf{A}\mathbf{x}\|^2\right). \tag{6}$$

The prior distribution corresponds to the previous information about the unknown coefficients. Assuming that the spectrum is smooth with respect to the directions and frequencies and defining the second order differences ε_{1mk} associated to direction $k$at frequency m and ε_{2mk} associated to the frequency m at the direction k as:

$$\begin{aligned} \varepsilon_{1mk} &= S(\omega_m,\theta_{k-1}) - 2S(\omega_m,\theta_k) + S(\omega_m,\theta_{k+1}) \\ \varepsilon_{2mk} &= S(\omega_{m-1},\theta_k) - 2S(\omega_m,\theta_k) + S(\omega_{m+1},\theta_k), \end{aligned} \tag{7}$$

the smoothness condition is equivalent to keeping the following summations as small as possible:

$$\sum_{k=1}^{K}\sum_{m=1}^{M} \varepsilon_{1mk}^2 = \mathbf{x^T H_1 x} \quad \text{with } S(\omega_m,\theta_0) = S(\omega_m,\theta_K) \quad \text{and}$$

$$S(\omega_m,\theta_{K+1}) = S(\omega_m,\theta_1) \tag{8}$$

$$\sum_{k=1}^{K}\sum_{m=2}^{M-1} \varepsilon_{2mk}^2 = \mathbf{x^T H_2 x} \tag{9}$$

where the matrices $\mathbf{H}_1$ and $\mathbf{H}_2$ may be easily constructed considering the proper definition of the vector $\mathbf{x}$. Furthermore, in order to avoid excessive spectral energy at frequency boundaries, the sum of the power of the spectrum is minimized in a pre-defined range of low and high frequencies given by $(\omega_1, \omega_2, \dots, \omega_L, \omega_H, \dots, \omega_M)$. For doing this, a third parameter is necessary, and it must be included in order restrain the estimations for frequencies in which both the RAO and the ship response are null. Considering the discretization of the problem, the following functional must be minimized (matrix $\mathbf{H}_3$ is obtained by a similar procedure used to derive $\mathbf{H}_1$ and $\mathbf{H}_2$):

$$\sum_{k=1}^{K}\sum_{m=1}^{L} S(\omega_m,\theta_k)^2 + \sum_{k=1}^{K}\sum_{m=H}^{M} S(\omega_m,\theta_k)^2 = \mathbf{x^T H_3 x}. \tag{10}$$

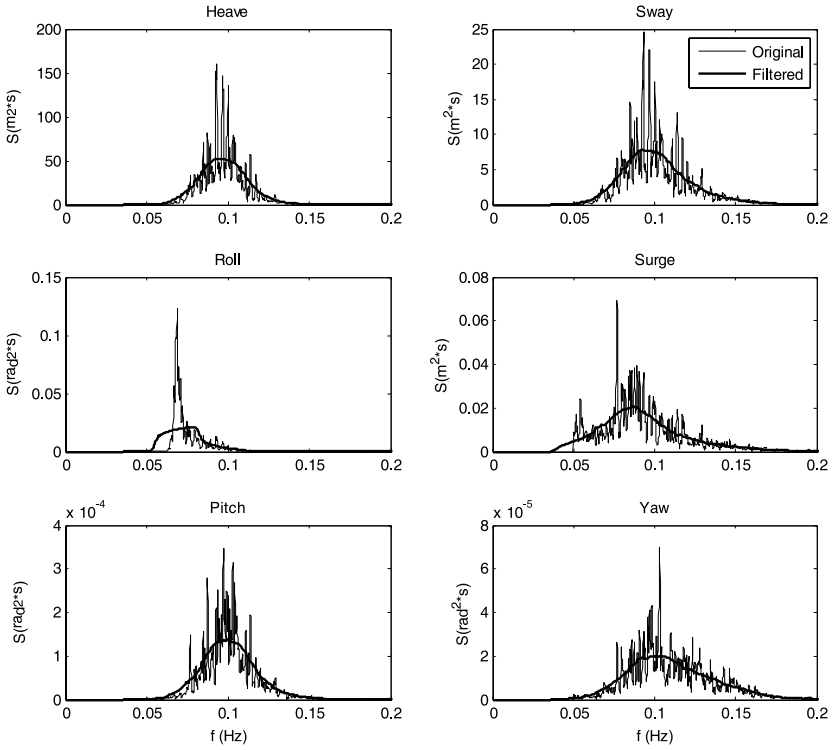

Fig. 2. Power spectrum estimation.

Table 1
FPSO main properties (real and model scales).

Properties	Real scale			Model scale (1:70)		
	Full	Intermediate	Ballasted	Full	Intermediate	Ballasted
Mass (M) (ton)	$2,667 \times 10^5$	$2,090 \times 10^5$	1.162×10^5	0.778	0.609	0.339
Moment of inertia (I_{xx}) ton m^2	9.39×10^7	6.30×10^7	5.79×10^7	5.29×10^{-2}	3.75×10^{-2}	3.12×10^{-2}
Moment of inertia (I_{yy}) ton m^2	1.72×10^9	1.36×10^9	9.49×10^8	1.02×10^0	8.12×10^{-1}	5.61×10^{-1}
Moment of inertia (I_{zz}) ton m^2	1.76×10^9	1.37×10^9	9.51×10^8	1.04×10^0	8.15×10^{-1}	5.66×10^{-1}
Length between perp. (Lpp) (m)		320			4.57	
Mean draft (T) (m)	18.44	14.73	8.51	0.263	0.210	0.122
Trim angle	0.41	0.80	0.48	0.41	0.80	0.48
Breadth (B) (m)		54.5			0.779	
Heave natural period (T_{n33}) (s)	11.7	11.0	10.0	1.40	1.32	1.20
Roll natural period (T_{n44}) (s)	14.7	13.4	12.6	1.76	1.61 s	1.51
Pitch natural period (T_{n55}) (s)	12.2	12.4	11.8	1.45	1.48	1.41

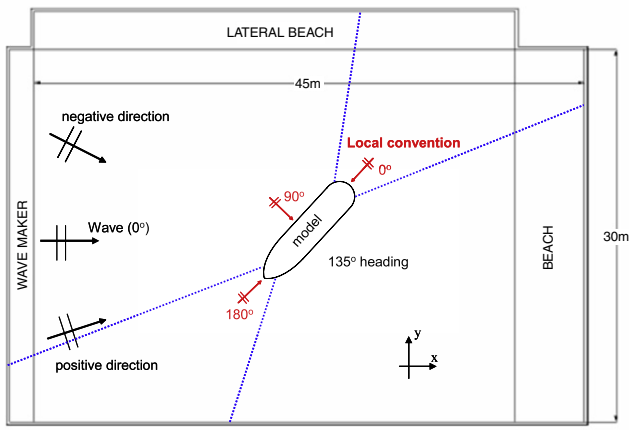

Fig. 3. LabOceano basin. Global (black) and Local (red, gray in print) reference systems for wave direction.

Considering that each of the prior distributions is a Gaussian variable, with zero mean and variances $\sigma^2/u_1^2; \sigma^2/u_2^2; \sigma^2/u_3^2$ for distributions (8)–(10) respectively, the product of likelihood function (6) by the overall prior distribution $p(\mathbf{x})$ is given by:

$$L(\mathbf{x}|\mathbf{B}) \cdot p(\mathbf{x}) = C \exp\left(-\frac{1}{2\sigma^2} \times \left(|\mathbf{B} - \mathbf{A}\mathbf{x}|^2 + \mathbf{x}^T(u_1^2\mathbf{H}_1 + u_2^2\mathbf{H}_2 + u_3^2\mathbf{H}_3)\mathbf{x}\right)\right) \quad (11)$$

with C being a factor independent of the model variable $\mathbf{x}$. The parameters u_1 and u_2 control the trade-off between good fit to the data and smoothness of the estimated spectrum in direction and frequency, respectively.

Finally, maximizing expression (11) is equivalent to minimizing the functional $J(\mathbf{x})$ given by:

$$J(\mathbf{x}) = |\mathbf{B} - \mathbf{A}\mathbf{x}|^2 + \mathbf{x}^T(u_1^2\mathbf{H}_1 + u_2^2\boldsymbol{H}_2 + u_3^2\boldsymbol{H}_3)\mathbf{x}. \quad (12)$$

Table 2
Parameters used in the Bayesian method.

	u_1	u_2	u_3	ω_L	ω_H
Ballasted	0.035	0.105	0.035	$2\pi/20$	$2\pi/6$
Intermediate	0.053	0.159	0.053	$2\pi/20$	$2\pi/6$
Loaded	0.070	0.210	0.070	$2\pi/30$	$2\pi/8$

A quadratic programming algorithm can then be used to perform the required minimization.

In most of the results presented ahead, the set of the hyperparameters was established *a priori*, after a sensitivity analysis. However, the ABIC criterion for defining the best choice of the hyperparameters u_1 and u_2 (as proposed by Nielsen [7]), was implemented and tested in some cases, as discussed in the next section. According to this criterion, the optimal values of (u_1, u_2) should be obtained by the numerical minimization of the following expression:

$$\mathrm{ABIC} = P \cdot \ln J(\mathbf{x}) - \ln\left|\det\left(u_1^2\boldsymbol{H}_1 + u_2^2\boldsymbol{H}_2\right)\right| + \ln\left|\det\left(\mathbf{A}\cdot\mathbf{A}^T + u_1^2\mathbf{H}_1 + u_2^2\mathbf{H}_2\right)\right| \quad (13)$$

where P is the total number of integral equations derived from Eq. (1).

3. Numerical implementation

The Bayesian Method was implemented using MATLAB 7.0®. Welch's method was used for the estimation of power and cross-spectra of motions from their time series. Each motion record was divided into eight sections with 50% overlap, each section being filtered by a Hanning window.

Figs. 1 and 2 show an example of motion record and the corresponding power spectra obtained by the Welch's method. A moving-average filter is applied (red lines in Fig. 2) in order to reduce the unevenness of the estimations. Furthermore, since the low frequency motions (due to the model's drifts) should not be taken into account in the spectrum estimation, a high-pass filter with 0.222 Hz cut-off frequency (corresponding to a cut-off period of 45 s) is also applied.

The following set of five motions was considered for the estimations: {surge, sway, heave, pitch, yaw}. Preliminary tests were performed with the triple {sway, heave, pitch} as suggested by Tannuri

Table 3
Set of waves for experimental tests at Labocean — theoretical values.

Test	Type	Wave parameters				
		H_s (m)	T_p (s)	Spreading factor s	Peakedness factor γ[a]	Direction (°)[b]
W90I1	Irregular	4.59	10.12	–	1.51	0
W90I2		8.05	14.56	–	1.70	0
W90I3		4.67	10.12	60	1.51	0
W90I4		4.63	10.12	12	1.51	0
W120B1	Bimodal	1.47(1) 0.98(2) 1.48(A)	11.54(1) 6.61(2) 11.40(A)	–	1.4(1) 0.9(2)	−30(1) 30(2)
W120B2		2.03(1) 0.70(2) 1.79(A)	7.28(1) 9.28(2) 7.30(A)	–	1.6(1) 2.0(2)	−30(1) 15(2)
W120B3		1.47(1) 0.63(2) 0.97(A)	5.35(1) 11.29(2) 11.40(A)	–	1.3(1) 2.2(2)	−30(1) 30(2)
W120B4		2.03(1) 0.98(2) 2.11(A)	11.46(1) 11.46(2) 11.40(A)	–	1.5(1) 1.2(2)	−30(1) 30(2)
W120B5		1.47(1) 0.98(2) 1.49(A)	11.54(1) 6.61(2) 11.40(A)	–	1.4(1) 0.9(2)	−30(1) −30(2)
W135I1	Irregular	4.59	10.12	–	1.51	0
W135I2		8.05	14.56	–	1.70	0
W135I3		4.67	10.12	60	1.51	0
W135I4		4.63	10.12	12	1.51	0
W150B1	Bimodal	1.47(1) 0.98(2) 1.48(A)	11.54(1) 6.61(2) 11.40(A)	–	1.4(1) 0.9(2)	−30(1) 30(2)
W150B2		2.03(1) 0.70(2) 1.79(A)	7.28(1) 9.28(2) 7.30(A)	–	1.6(1) 2.0(2)	−30(1) 15(2)
W150B3		1.47(1) 0.63(2) 0.97(A)	5.35(1) 11.29(2) 11.40(A)	–	1.3(1) 2.2(2)	−30(1) 30(2)
W150B4		2.03(1) 0.98(2) 2.11(A)	11.46(1) 11.46(2) 11.40(A)	–	1.5(1) 1.2(2)	−30(1) 30(2)
W150B5		1.47(1) 0.98(2) 1.49(A)	11.54(1) 6.61(2) 11.40(A)	–	1.4(1) 0.9(2)	−30(1) −30(2)

[a] Here we assume a JONSWAP spectrum type.
[b] Global (tank) coordinate system.

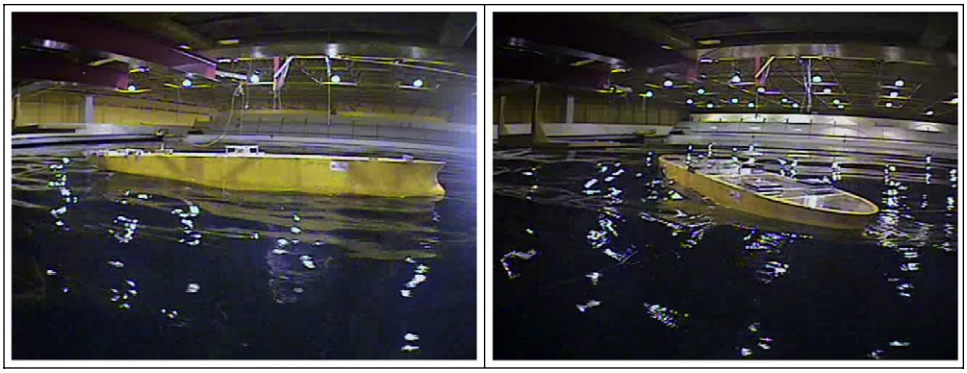

Fig. 4. Views of the P35 model during tests (a) ballast condition — 90° heading; (b) Full load condition — 135° heading.

et al. [2], roll motion being excluded due to the inherent uncertainties regarding its transfer function, as explained before. Nevertheless, additional tests later indicated that by including surge and yaw records a slight improvement in the estimations was generally obtained without a significant increase in computational time.

The transfer functions of motions were obtained using a well-known wave-body interaction BEM code (WAMIT®, [13]). Based on the model's hull geometry, numerical meshes were constructed for each one of the loading conditions, also considering their respective trim angles specified in Table 1.

The ABIC criterion for defining the best choice of the hyperparameters u_1 and u_2 was tested in some situations and provided good results (examples will be given below). However, this procedure was extremely time-consuming and therefore considered impractical for real on-board estimations. A different procedure was then employed, where the parameters were previously calibrated for each loading condition using exhaustive numerical analysis and experimental results. A fixed set of values was then pre-defined for each draft and adopted for all the tests. These values are given in Table 2.[1] As a general result, it could be inferred that the sensitivity of the estimations to variations in these parameters decreases with the level of response. As a consequence, estimations based on the response of the model in full-loading condition were more susceptible to errors caused by the wrong choice of the hyperparameters.

4. Experimental setup

Model tests were carried out in the LabOceano facilities, in Rio de Janeiro. Its 45 m long, 30 m wide, 15 m deep wave basin is able to generate multi-directional waves through an in-line array of 75 flap-type wavemakers that allows emulating short-crested seas with variable spreading or the combination of two different long-crested seas. Fig. 3 shows a sketch of the LabOceano basin and the coordinate systems adopted for the analysis. Directional wave spectra will be presented in two different patterns: in a polar plot with directions relative to the vessel model ("local reference system" — 180° denoting bow incidence) and also in the basin-fixed reference frame (0° denoting waves that propagate perpendicular to the wavemakers, towards the opposite beach).

Wave calibration tests were performed in the absence of the FPSO model and the evaluation of the directional wave spectrum within the test zone was performed by means of a wave probe array. The standard procedure adopted by LabOceano for measuring directional waves follows Stansberg [11], making use of an array of eight wave probes and applying the Maximum Entropy Method (MEM) for the spectrum evaluation. The set of wave spectra obtained in the calibration tests represents the standard to which the estimations based on ship motions are compared. A full description of the wave calibration procedure is given in Tannuri et al. [12].

The hull of the P-35 FPSO model was built in 1:70 scale and tested in three different mean drafts, corresponding to a ballast condition ($T = 8.51$ m), an intermediate load situation ($T = 14.73$ m) and a full load condition ($T = 18.44$ m). The main characteristics of the vessel in the three different conditions are presented in Table 1, both in real and in model scale. Each load condition was tested with a corresponding trim angle, derived from the FPSO loading and stability reports. One may readily see in Table 1 that the trim can reach considerable values, especially in the intermediate load condition. Fig. 4 shows two views of the FPSO model during tests in ballast (a) and full-load (b) conditions. In order to simplify the tests, the mooring line arrangement adopted was composed of four horizontal springs designed for the unique purpose of keeping heading variations and model offsets within reasonable limits. A sketch of the mooring arrangement may be seen in Fig. 3 (dotted lines).

Irregular wave tests were performed for intervals corresponding to 3 h in real scale, during which the motions of the vessel in 6 d.o.f were measured by means of an optical device. Motions were subsequently transferred to the CG position, with respect to which the RAOs were derived, as explained in the preceding section. Fig. 5 shows examples of the RAOs derived for the FPSO model (surge and pitch RAOs in head waves; sway and roll in beam waves and yaw in quartering waves) in the three different loading conditions (periods in full-scale). Although not included in the estimation procedure, roll RAOs are also presented for completeness, and were derived considering typical viscous damping factors for each loading condition.

The whole set of waves tested is listed in Table 3 (all values in full-scale). Here, four main groups of tests can be distinguished. The first group of experiments (W90IX) corresponds to beam-sea (incidence of 90° with respect to the vessel local coordinate system) unimodal waves. The vessel heading is 90° in the LabOceano coordinate system. Tests $X = 1, 3, 4$ have the same height and period, but increasing directional spreading. Values of height and period correspond to a typical 1 yr-return condition, according to Campos Basin metocean data. Test $X = 2$ represents the worst 100 yr condition in the Campos Basin. The same pattern is adopted in the third group of experiments (W135IX), which is

[1] Frequencies (ω_L, ω_H) were defined by a qualitative analysis of the RAOs.

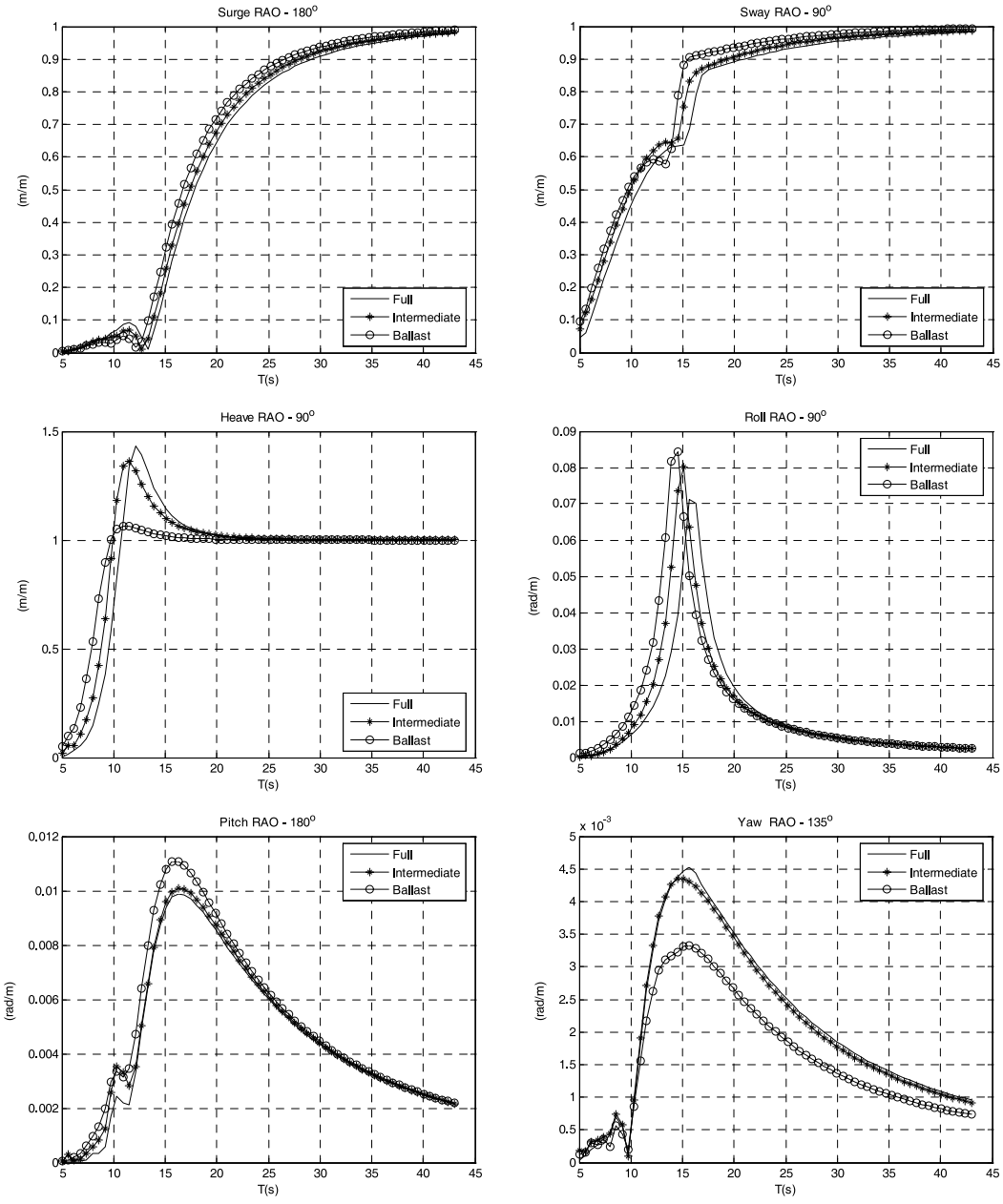

Fig. 5. FPSO RAOs.

equivalent to the first set, but now with an incidence angle of 135° related to the vessel coordinate system (vessel heading of 135° in the basin).

The second group of experiments in Table 3, labeled as W120BX, consists of bimodal sea states. These waves were generated in the tank by the composition of two long-crested seas with different heights, periods and directions. In these cases, the table specifies H_S and T_P for both components (indicated by (1) and (2)) and also their average (combined) values (A), as computed by the Maximum Entropy Method from the measurements in the tank. The aperture angle between wave directions is 60° (+30° and −30° in the tank system) for the tests $X = 1$, 3, 4 and 45° for $X = 2$. The test $X = 5$ combines two wave components with different peak periods, but coming from the same direction. For all the tests in this group, the vessel heading is 120° in the LabOceano coordinate system. Finally, the fourth group (W120BX) consists of tests with the same waves of the second group, but now with a vessel heading of 150° in the tank coordinate system.

All the wave conditions reported in Table 3 were tested for the three different loadings of the FPSO model. The next section discusses how statistical wave parameters estimated from model motions compare to the reference values of Table 3, for each loading condition. Different aspects of the estimation model such as filtering of high frequency components, the influence of zeros in the transfer functions, the use of the ABIC criterion vis-à-vis calibration of the hyperparameters are discussed based on illustrative results.

5. Motion-based estimations and comparisons

All the wave tests were run with the FPSO model in the three different draft conditions and the results estimated by means of the Bayesian inference method were directly compared to the

Table 4
Experimental results of the Bayesian estimation — ballasted condition (P35B).

Test	Experimental			Bayesian — $u_1 = u_3 = 0.035\ u_2 = 3 * 0.035$			Errors		
	H_s (m)	T_p (s)	Dir (°)	H_s (m)	T_p (s)	Dir (°)	H_s (%)	T_p (%)	Dir (°)
P35B90I1	4.59	10.12	89.87	3.99	11.42	82.56	−13.1	12.8	−7.3
P35B90I2	8.05	14.56	91.08	7.48	13.96	86.79	−7.1	−4.1	−4.3
P35B90I3	4.67	10.12	90.70	4.50	9.67	90.23	−3.5	−4.5	−0.5
P35B90I4	4.63	10.12	92.48	4.92	10.47	108.67	6.1	3.4	16.2
P35B120B1	1.48	11.40	117.95	1.50	10.47	124.51	1.7	−8.2	6.6
P35B120B2	1.79	7.30	107.57	1.61	7.85	108.01	−10.0	7.7	0.4
P35B120B3	0.97	11.40	120.39	0.73	10.47	140.72	−25.4	−8.2	20.3
P35B120B4	2.11	11.40	118.70	2.23	10.47	127.23	5.3	−8.2	8.5
P35B120B5	1.49	11.40	105.04	1.55	11.42	110.59	4.0	0.2	5.6
P35B135I1	4.59	10.12	134.87	4.31	10.47	148.13	−6.1	3.4	13.3
P35B135I2	8.05	14.56	136.08	8.05	13.96	139.17	0.0	−4.1	3.1
P35B135I3	4.67	10.12	135.70	4.35	9.67	145.92	−6.8	−4.5	10.2
P35B135I4	4.63	10.12	137.48	4.28	9.67	142.06	−7.7	−4.5	4.6
P35B150B1	1.48	11.40	147.95	1.41	10.47	143.26	−4.4	−8.2	−4.7
P35B150B2	1.79	7.30	137.57	1.22	7.85	146.10	−31.8	7.7	8.5
P35B150B3	0.97	11.40	150.39	0.61	10.47	172.43	−36.8	−8.2	22.0
P35B150B4	2.11	11.40	148.70	2.14	10.47	146.57	1.4	−8.2	−2.1
P35B150B5	1.49	11.40	135.04	1.52	10.47	136.73	1.8	−8.2	1.7

Table 5
Experimental results of the Bayesian estimation — intermediate condition (P35I).

Test	Experimental			Bayesian — $u_1 = u3 = 0.053\ u_2 = 0.159$			Errors		
	H_s (m)	T_p (s)	Dir (°)	H_s (m)	T_p (s)	Dir (°)	H_s (%)	T_p (%)	Dir (°)
P35I90I1	4.59	10.12	89.87	4.87	9.67	92.04	6.1	−4.5	2.2
P35I90I2	8.05	14.56	91.08	8.27	15.71	91.91	2.8	7.9	0.8
P35I90I3	4.67	10.12	90.70	5.61	8.98	109.22	20.1	−11.3	18.5
P35I90I4	4.63	10.12	92.48	6.11	8.98	116.97	31.8	−11.3	24.5
P35I120B1	1.48	11.40	117.95	1.77	8.98	136.82	19.7	−21.3	18.9
P35I120B2	1.79	7.30	107.57	1.44	8.38	99.97	−19.1	14.8	−7.6
P35I120B3	0.97	11.40	120.39	0.72	9.67	134.15	−26.3	−15.2	13.8
P35I120B4	2.11	11.40	118.70	2.53	9.67	138.87	19.6	−15.2	20.2
P35I120B5	1.49	11.40	105.04	1.80	8.98	127.70	20.6	−21.3	22.7
P35I135I1	4.59	10.12	134.87	3.48	10.47	139.95	−24.2	3.4	5.1
P35I135I2	8.05	14.56	136.08	7.86	13.96	134.29	−2.4	−4.1	−1.8
P35I135I3	4.67	10.12	135.70	4.16	9.67	132.86	−10.8	−4.5	−2.8
P35I135I4	4.63	10.12	137.48	4.61	9.67	135.88	−0.5	−4.5	−1.6
P35I150B1	1.48	11.40	147.95	1.43	10.47	147.54	−2.9	−8.2	−0.4
P35I150B2	1.79	7.30	137.57	0.93	8.38	126.15	−48.1	14.8	−11.4
P35I150B3	0.97	11.40	150.39	0.57	10.47	174.35	−41.5	−8.2	24.0
P35I150B4	2.11	11.40	148.70	2.20	9.67	151.24	4.1	−15.2	2.5
P35I150B5	1.49	11.40	135.04	1.55	10.47	142.96	3.9	−8.2	7.9

Table 6
Experimental results of the Bayesian estimation — loaded condition (P35L).

Test	Experimental			Bayesian — $u_1 = u_3 = 0.07\ u_2 = 0.21$			Errors		
	H_s (m)	T_p (s)	Dir (°)	H_s (m)	T_p (s)	Dir (°)	H_s (%)	T_p (%)	Dir (°)
P35L90I1	4.59	10.12	89.87	4.41	9.67	92.16	−4.0	−4.5	2.3
P35L90I2	8.05	14.56	91.08	8.15	15.71	88.98	1.2	7.9	−2.1
P35L90I3	4.67	10.12	90.70	4.86	9.67	79.39	4.1	−4.5	−11.3
P35L90I4	4.63	10.12	92.48	5.33	9.67	74.19	14.9	−4.5	−18.3
P35L120B1	1.48	11.40	117.95	1.50	9.67	116.39	1.4	−15.2	−1.6
P35L120B2	1.79	7.30	107.57	1.06	8.38	85.49	−40.9	14.8	−22.1
P35L120B3	0.97	11.40	120.39	0.67	10.47	126.99	−30.6	−8.2	6.6
P35L120B4	2.11	11.40	118.70	2.22	9.67	125.02	5.1	−15.2	6.3
P35L120B5	1.49	11.40	105.04	1.53	9.67	117.02	2.4	−15.2	12.0
P35L135I1	4.59	10.12	134.87	3.67	10.47	114.96	−20.0	3.4	−19.9
P35L135I2	8.05	14.56	136.08	7.94	15.71	128.64	−1.4	7.9	−7.4
P35L135I3	4.67	10.12	135.70	3.91	9.67	103.66	−16.3	−4.5	−32.0
P35L135I4	4.63	10.12	137.48	4.04	9.67	112.97	−12.8	−4.5	−24.5
P35L150B1	1.48	11.40	147.95	1.42	10.47	136.10	−3.6	−8.2	−11.8
P35L150B2	1.79	7.30	137.57	0.67	8.98	105.24	−62.6	23.0	−32.3
P35L150B3	0.97	11.40	150.39	0.51	10.47	174.13	−47.8	−8.2	23.7
P35L150B4	2.11	11.40	148.70	2.16	10.47	138.76	2.4	−8.2	−9.9
P35L150B5	1.49	11.40	135.04	1.58	10.47	127.36	6.1	−8.2	−7.7

P35B90I1	Experimental	Bayesian	Errors
Hs (m)	4.59	3.99	-13.1%
Tp (s)	10.12	11.42	12.8%
Direction (°)	89.87	82.56	-7.3°

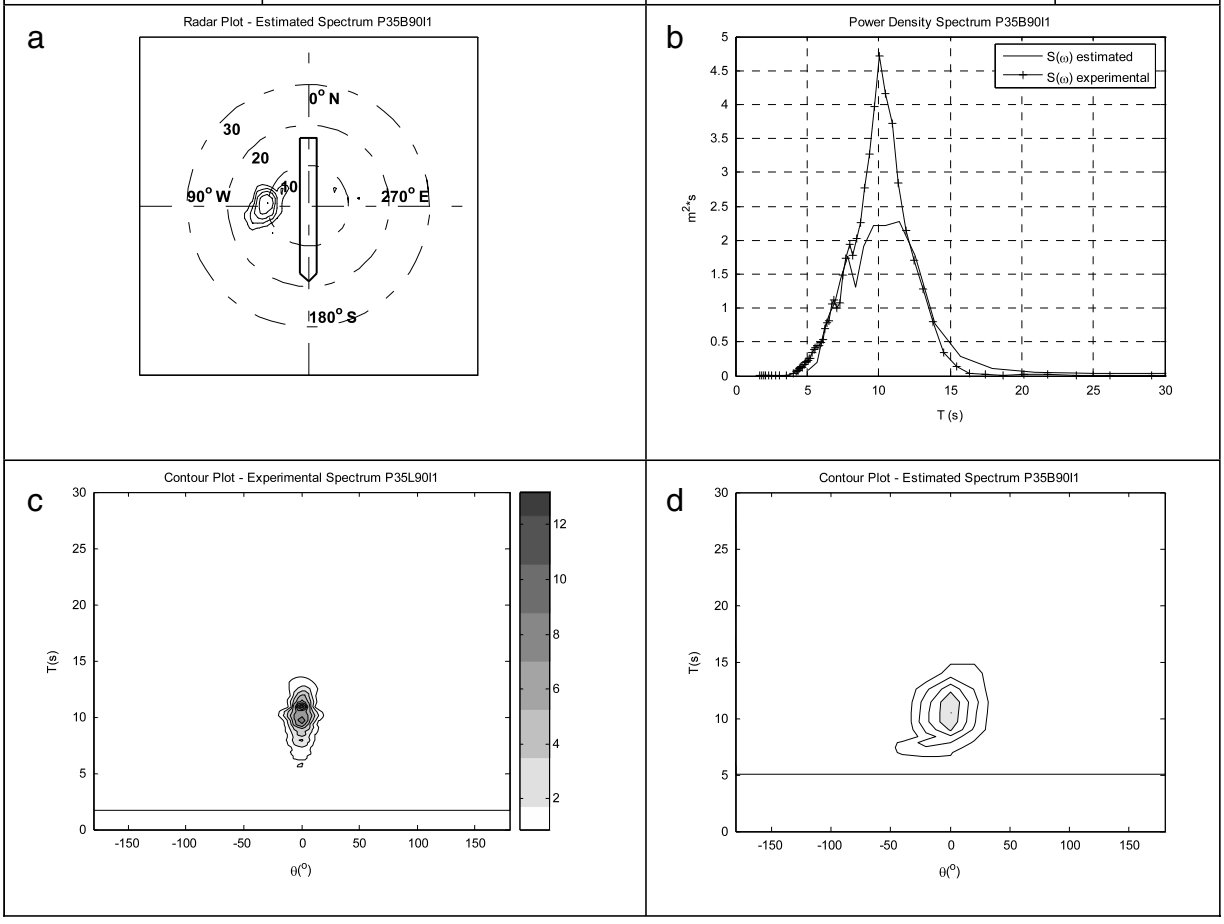

Fig. 6. Experimental results — P35B90I1 test.

parameters obtained in the wave calibration process, presented in Table 3. The whole set of results is presented in three tables: Table 4 presents the results for the ballasted FPSO (P35BX); Table 5 refers to the FPSO in intermediate condition (P35IX) and, finally, Table 6 contains the results for the loaded FPSO (P35LX). It should be noticed that wave directions refer to the local reference system or, in other words, directions are given relative to the ship heading. Also, estimations concerning combined (sea + swell) sea states (the bimodal tests) all refer to average values concerning the combined spectra.

As explained before, a unique set of values of the hyperparameters was adopted for each one of the loading conditions (see Table 2 [12]). Values were defined by means of a "calibration" process bases on numerical simulations, searching for those who resulted in minimum errors concerning the average of all tests. This process showed that such errors are almost insensitive to the hyperparameters when the model is in ballast conditions, and tend to become more sensitive as the loading increases. This is obviously related to the levels of the dynamic response to waves, which decreases with the model draft. A more robust alternative would be to search for the best values of the parameters for each one of the tests, using for example the ABIC criterion. Examples of this procedure will be discussed later in this paper.

Results indeed indicate an overall good agreement between Bayesian estimated spectra and those obtained from the wave probe measurements. Mean errors in the statistical parameters considering all tests are shown in Table 7. The maximum mean errors observed in H_S and T_P were obtained for the model in an intermediate loading condition. In this case, these errors were approx 17% and 11%, respectively. It is interesting to observe that, contrary to what could be anticipated, the corresponding errors in full loading condition were slightly smaller (with the exception of the error in mean direction). This is probably connected to specificities of the RAOs (this condition presents the highest trim angle, intensifying the bow-stern asymmetry) and also, eventually,

P35B90I3	Experimental	Bayesian	Errors
Hs (m)	4.67	4.50	-3.5%
Tp (s)	10.12	9.67	-4.5%
Direction (°)	90.70	90.23	-0.5°

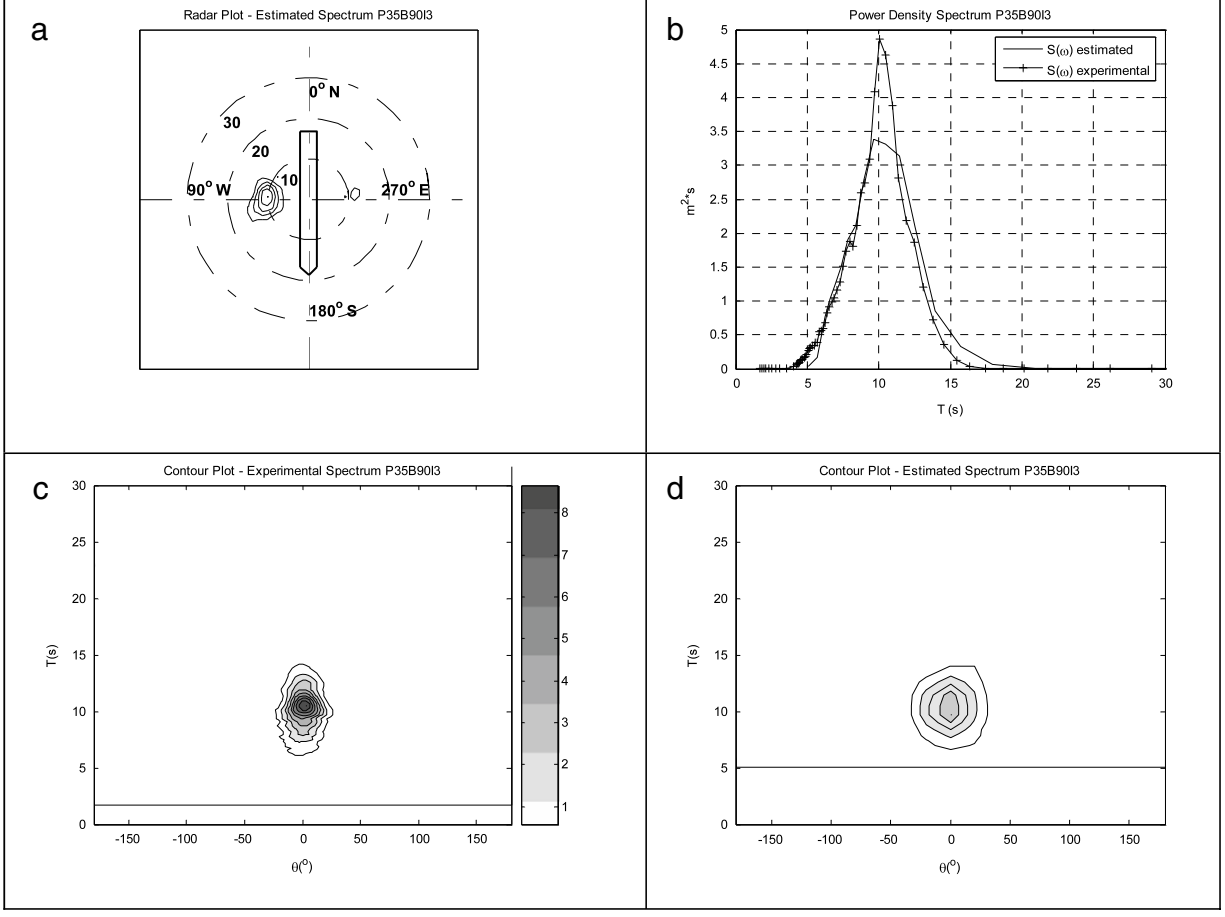

Fig. 7. Experimental results — P35B90I3 test.

Table 7
Mean errors in statistical parameters for each loading case.

	Mean absolute errors		
	H_s (%)	T_p (%)	Dir (°)
Ballasted	9.6	6.3	7.8
Intermediate	16.9	10.8	10.4
Loaded	15.4	9.2	14.0

with the choice of fixed values of the calibration parameters. Nevertheless, it should be observed that the mean errors are quite acceptable for all three drafts.

Analysis of the whole set of results shows that in some cases errors significantly above the mean values were obtained, especially for two bimodal sea conditions B2 and B3. Errors in the estimation of these wave conditions increase with the draft and reach very high levels for intermediate and full-load conditions. In fact, these errors could be anticipated and are mostly associated with the filtering of high-frequency wave components. These and other illustrative results that throw some light on important aspects of the methodology will be discussed in more detail next.

As a first example, Fig. 6 presents the results for the test P35B90I1. In this test, according to Table 3, the wave condition corresponds to a long-crested sea that reaches the vessel in a beam sea condition (90° to the hull). Fig. 6 presents: a contour plot of the estimated spectrum with directions respective to the vessel heading (a); a comparison of estimated (Bayesian) and experimental power spectra (b) and the spectrum maps (c) and (d) depicted in the wave tank reference system (according to Fig. 3). Please notice that (c) and (d) share the same colorbar scale, since the interval of contour lines is the same for both maps. In this case, errors in H_S, T_P and direction were approximately $\{-13\%; 13\%; -7.3°\}$, respectively. Similar errors were obtained for situations with increasing directional spreading. This can be seen

P35B150B5	Experimental	Bayesian	Errors
Hs (m)	1.49	1.52	1.8%
Tp (s)	11.40	10.47	-8.2%
Direction (°)	135.04	136.73	1.7°

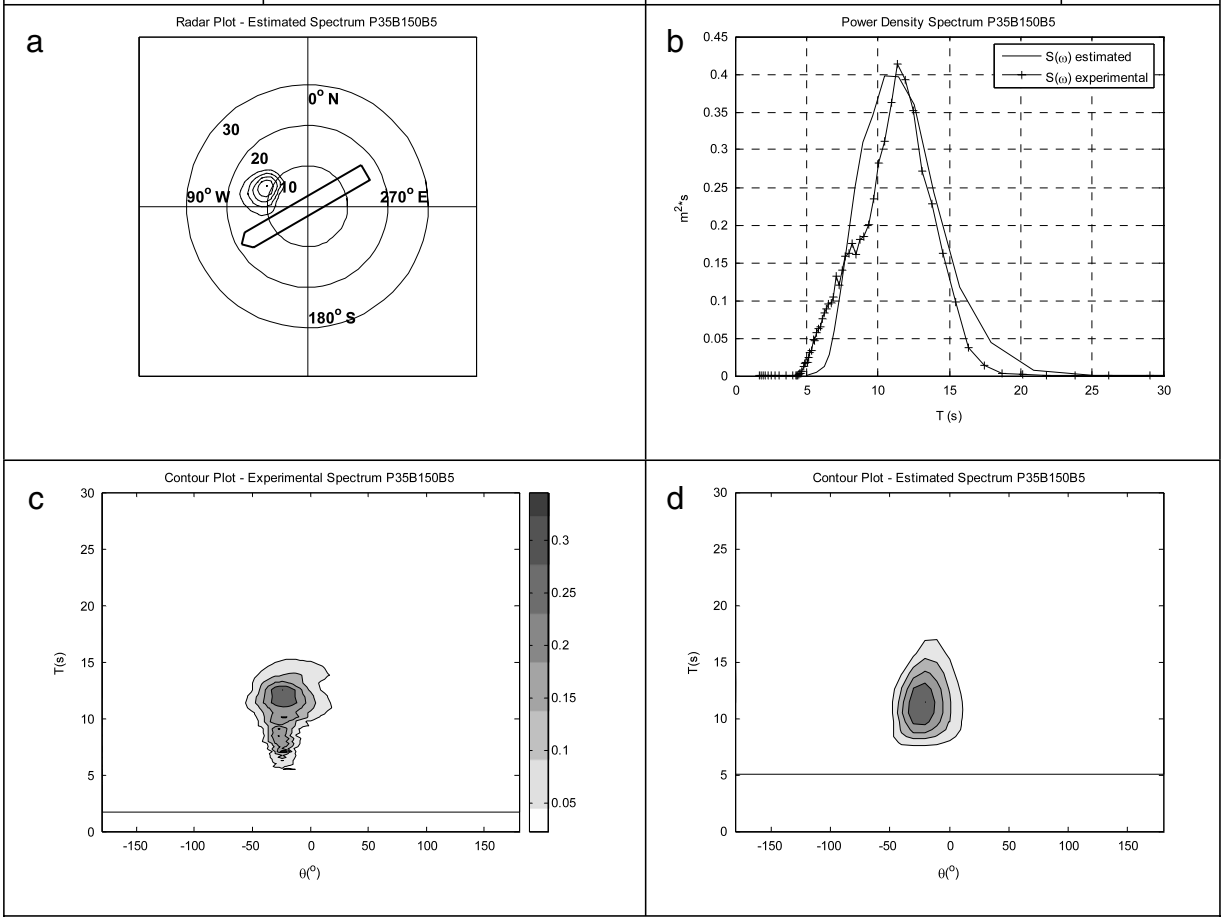

Fig. 8. Experimental results — P35B150B5 test.

by comparing these errors to those obtained in cases P35B90I3-4, tests with the same H_S and T_P but with larger directional spreading. For the sake of comparison, results from test P35B90I3 are presented in Fig. 7, following the same standard discussed above.

More demanding problems are posed by the tests with bimodal wave spectra, generated by means of the superposition of two long-crested seas in the wave basin. For starting the discussion on these results, let us consider the case when both waves come from the same direction (wave W150B5 in Table 3 [12]). This situation is composed by a quite mild sea condition, with an average wave height of approximately 1.5 m and the wave spectrum has two peaks with quite different periods, one around 11.5 s and the other close to 6.6 s, this last one below the estimated cut-off period imposed by the vessel (estimated to be around 7.0 s). For illustrating the results, Fig. 8 presents the estimations concerning test P35B150B5. In this case, the waves hit the vessel with a mean angle of 30° from its bow. It is interesting to see that, as most of the wave energy is concentrated in the sea with higher peak period, both the wave height and mean period are well captured, although the cut-off of high frequency components below 7 s is clear in (d), where the smaller wave component is missed. Errors on the average statistical parameters in this case are indeed quite small (1.8% for H_S, −8.2% for T_P and 1.7° in direction). Obviously, the errors should increase with the vessel draft, since motions become smaller and the cut-off period tends to increase. The increase in the errors can be observed by comparing Tables 3–5. To exemplify this issue, the estimations for the same wave condition obtained with the fully-loaded model (test P35L150B5) are depicted in Fig. 9. Compared to the case in the ballast condition, the deterioration of the estimated spectrum is clear, with a slight tendency of spreading the energy towards the bow of the vessel. As will be discussed later, this trend was observed in some cases and it is connected to the some particularities of the

P35L150B5	Experimental	Bayesian	Errors
Hs (m)	1.49	1.58	6.1 %
Tp (s)	11.40	10.47	-8.2 %
Direction (°)	135.04	127.36	-7.7°

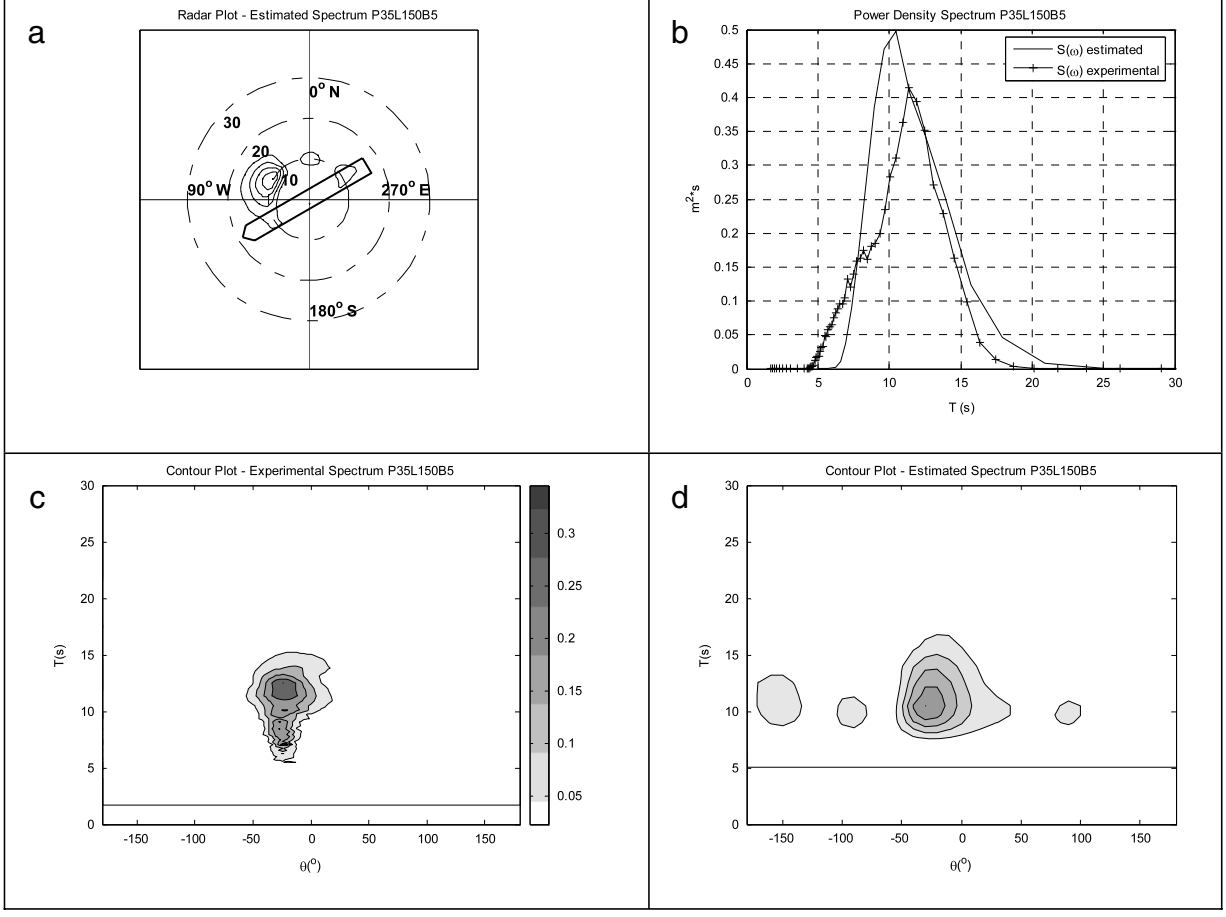

Fig. 9. Experimental results — P35L150B5 test.

RAOs. Nevertheless, this spread of energy, although deforming the wave map, is not quite significant in terms of total energy and, as a consequence, the error in the mean direction remains below 8°. Results are indeed quite impressive, if one reminds that these mild waves are estimated from the motions of a loaded VLCC.

Next, some considerations will be made concerning the tests with higher errors on the estimations, as for example the tests with wave W150B3. In this case, the error in H_S predictions reaches values close to −50% in the fully-loaded condition (see Table 6 [12]). A quick evaluation of the wave conditions makes it evident that this test was indeed designed to exemplify the kind of situation that will impose the most severe problems to the motion-based estimations. In fact, in this case two combined waves occur, coming from directions with an aperture angle of 60°. A higher wave (1.47 m) with a quite low period (5.3 s) encounters the vessel from an angle of 30° from the bow, while a small swell (only 0.6 m high with a peak period of 11.3 s) hits the vessel from the bow. Fig. 10 depicts the results for the model in ballast condition and it is clear that the wave component with higher frequencies is overlooked, since most of its energy is filtered by the vessel. As a consequence, only the lower frequency wave component is "identified" and this leads to errors also in the mean direction, of approx 20°. Obviously, these errors tend to increase with the model loading. This kind of situation is illustrative of the limitations imposed from estimating the waves from the motions of such a large vessel. For estimating high frequency wave components, smaller vessels would be preferable. On the other hand, it is interesting to observe that the errors obtained when estimating the same sea condition are smaller for the other vessel heading (120), in the cases P35X120B3, since, in these cases, although the higher wave component is once again missed, the waves hit the vessel with larger angles from the bow and this is favorable for increasing the vessel

P35B150B3	Experimental	Bayesian	Errors
Hs (m)	0.97	0.61	-36.8%
Tp (s)	11.40	10.47	-8.2 %
Direction (°)	150.39	172.43	22.0°

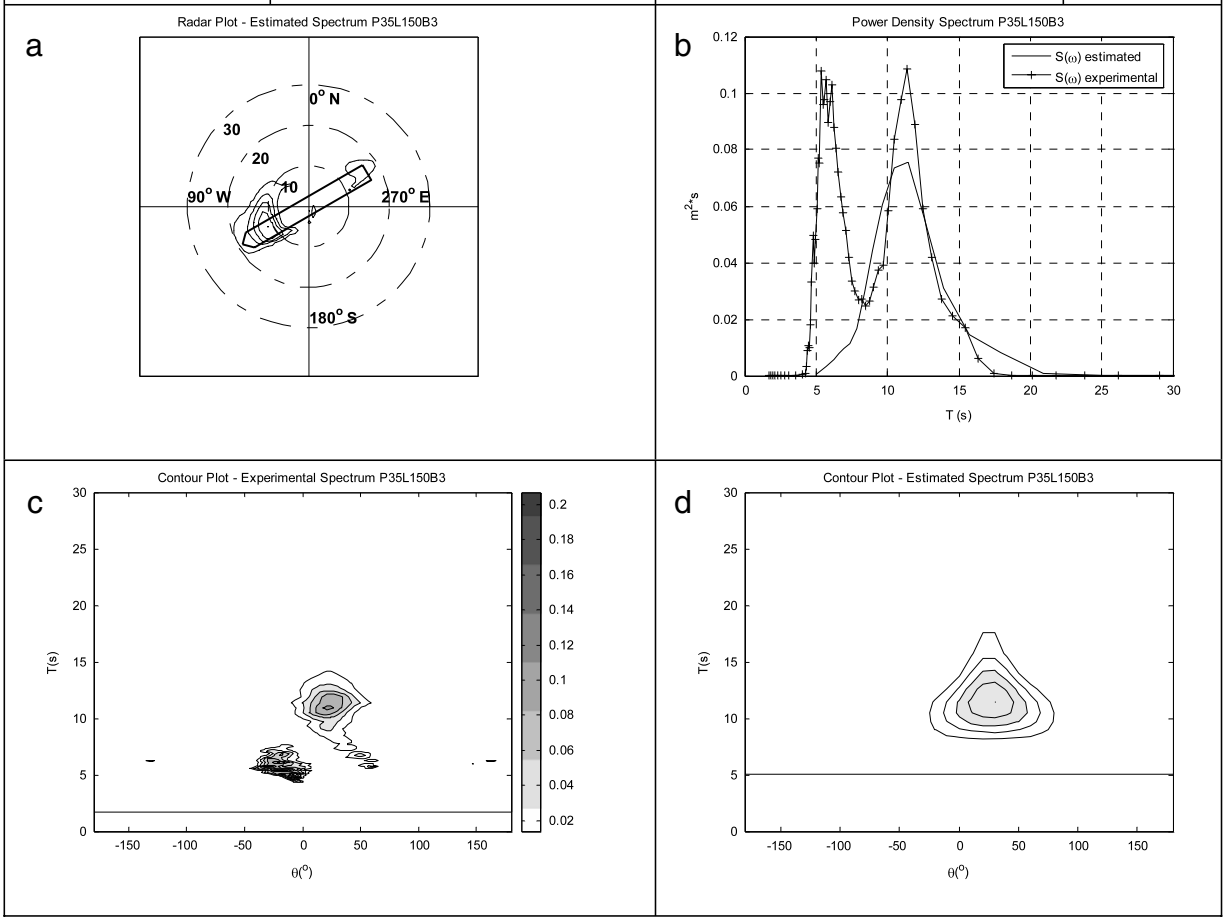

Fig. 10. Experimental results — P35B150B3 test.

motions. Fig. 11 presents the results for the case P35B120B3 and, by comparing its results to those of Fig. 10, one may see that the spectrum with a higher period is now estimated more accurately.

Finally, it was already commented on that a tendency to spread part of the energy towards the vessel bow was observed in some situations. This trend is connected to particularities of the vessel response and may be amplified by an inadequate choice of the hyperparameters. This is more evident for the medium and full-load drafts and may be quite well illustrated by Fig. 12, relative to the test P35L120B5. In this specific case, the hyperparameter u_2 was changed to 0.07 in order to make the problem more visible. Errors in the estimations are respectively 9.5% and −15.2% for height and period and 25.4° for the mean direction. The spread of energy towards the bow around the peak period of the spectrum is clear. The reason for this spurious behavior is connected to the transfer function of motions. To illustrate this point, Fig. 13 presents the heave and pitch RAOs of the model in loaded condition for three different angles of incidence (180°, 135° and 90°), therefore, from head to beam waves. First of all, it should be noticed that the vessel presents some significant pitch response in beam waves and this in not only due to the bow-stern asymmetry of the hull, but also due to the trim angle, which in this case is 0.41° (see Table 1). Also, it can be seen that the heave motion in 180° (bow incidence) presents almost no-response for periods smaller than 10 s and that in this period an almost complete cancelation of the response occurs. One should notice that in this case this period is very close to the peak period of the waves that are reaching the vessel in 90° (T_p = 11.5 s, see Table 3). These characteristics of the response therefore impose a difficult situation to the estimation model, since the pitch response (that really exists around beam incidence) may also be represented around the bow incidence without significantly affecting the heave response for periods close to the peak period of

P35B120B3	Experimental	Bayesian	Errors
Hs (m)	0.97	0.73	-25.4%
Tp (s)	11.40	10.47	8.2%
Direction (°)	120.39	140.72	20.3°

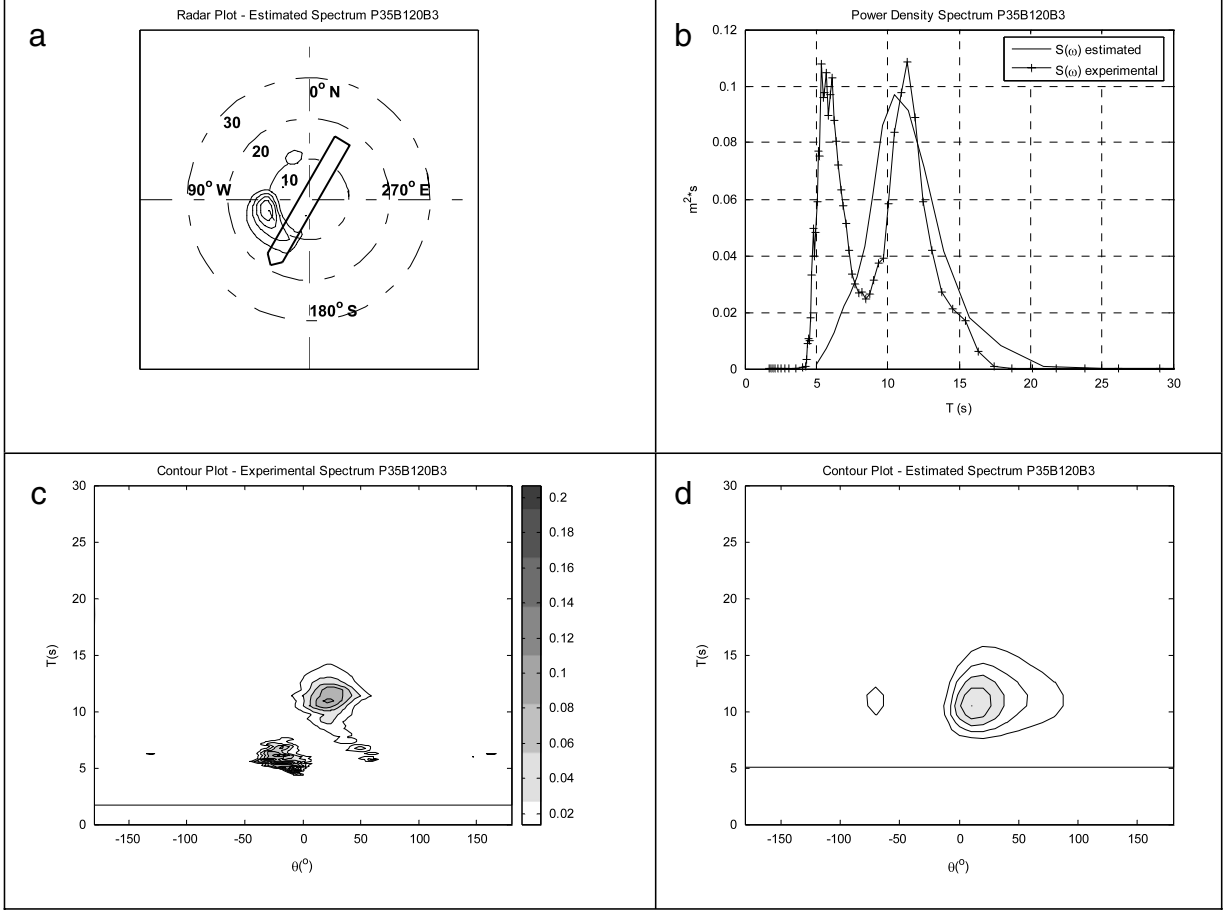

Fig. 11. Experimental results — P35B120B3 test.

the wave spectrum. That explains the trend to spread the estimated wave spectrum towards the bow and, as a result, the estimated spectrum overestimates the wave energy around the peak period. A few comments on this behavior must be made in this point: first of all, the problem happens for a small range of frequencies around the "cancelation" point of heave response and therefore, contrary to the expectations expressed by Pascoal et al. [8], it does not make the vessel a "very poor estimator". Indeed, the errors in the statistics remain quite acceptable, considering all of the difficulties involved in this sort of estimation. Furthermore, it seems possible to minimize or even eliminate this error by choosing the hyperparameters correctly. As explained before, for the Bayesian methodology involving two hyperparameters (u_1 and u_2), the use of the ABIC criterion would be desirable in order to determine their values. Nevertheless, this procedure should be adopted for each estimate and it was not followed in this work for purely practical reasons, since one is mainly concerned here with the applicability of the method for on-board estimations. Therefore, a previously "calibrated" set of values of u_1 and u_2 (and also u_3) was kept fixed for each loading condition, guaranteeing quite expeditious estimations. However, for the sake of illustrating this point, the application of the ABIC criterion was tested and, regarding the test above, the improvement is clear. The map of the ABIC values is depicted in Fig. 14 and the point of minimum value corresponds to ($u_1 = 0.075$ and $u_2 = 0.168$). Results of the same wave test obtained when using this set of hyperparameters are presented in Fig. 15. One can readily see that the tendency of spreading energy towards the bow is now restricted by the imposition of a sufficiently smooth distribution in frequency (controlled by the parameter u_2) and the errors in the estimations are reduced to 1.9% in the wave height and 13° in the mean wave direction.

In summary, from the whole set of tests performed, it is possible to infer that accurate estimations may be obtained based on the

T21_70300	Experimental	Bayesian	Errors
Hs (m)	1.49	1.63	9.5%
Tp (s)	11.40	9.67	-15.2%
Direction (°)	105.04	130.46	25.4°

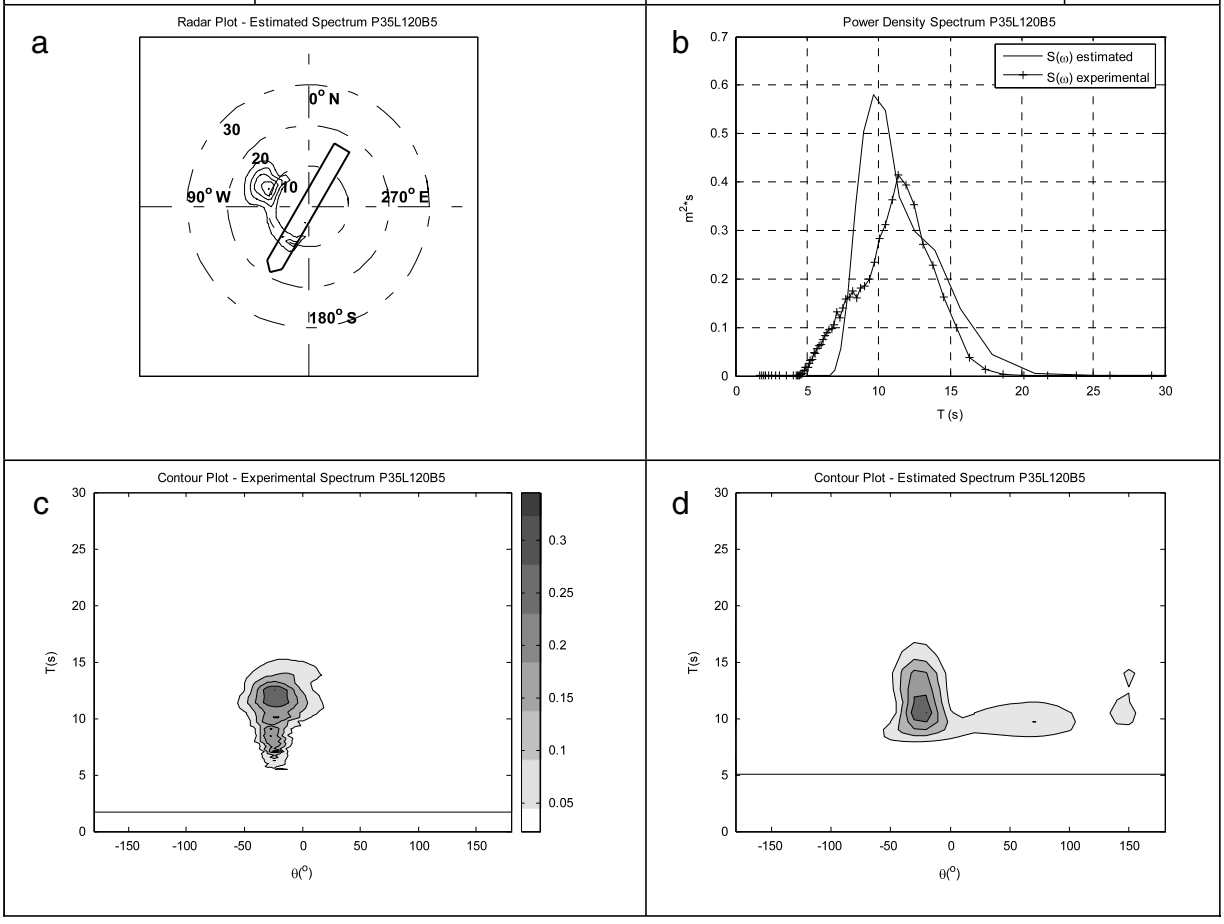

Fig. 12. Experimental results — P35L120B5 test.

vessel motions (even considering a large one, such as a VLCC), provided that a significant amount of wave energy is not filtered by the vessel. Also, one may foresee that the on-board results may be even further refined if a criterion such as the ABIC can be numerically implemented in a way that is not prohibitively time-consuming.

6. Conclusions

The feasibility of employing an FPSO hull for motion-based estimations of the wave spectrum was analyzed by means of an extensive set of small-scale tests performed in a wave basin. For this task, a (1:70) small-scale model of the P-35 platform was tested in three representative loading situations. In order to evaluate the limitations of the methodology, the selection of wave conditions included typical sea conditions measured in the Campos Basin/Brazil and also conditions pre-defined for testing some of its possible drawbacks. Long and short crested seas and also combined (sea + swell) conditions were emulated in the tank. The spectra estimated from the model's motions were confronted to those obtained from the measurements performed by an array of eight wave-probes, employing MEM.

A Bayesian inference model with two hyperparameters (as proposed by Nielsen [7]) was adopted for the estimations. A previous analysis showed that the addition of the second hyperparameter indeed improved the results, compared to those obtained with a single one. Also, following Tannuri et al. [2], roll motion was discarded for the analysis due to the inherent inaccuracies involved in the prediction of its transfer function (RAO). It was also verified that the estimations based on all the other five motions (including surge and yaw) promoted a slight improvement of the results, compared to those obtained from the usual sway-heave-pitch set, and did not represent any significant increase in terms of computational effort.

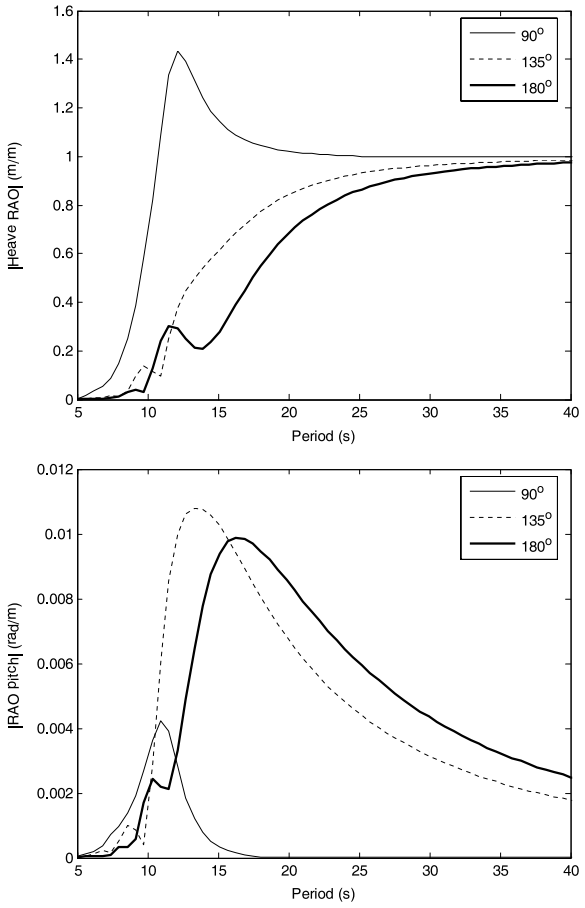

Fig. 13. Heave and Pitch RAOs — Model in fully-loaded condition (periods in full scale).

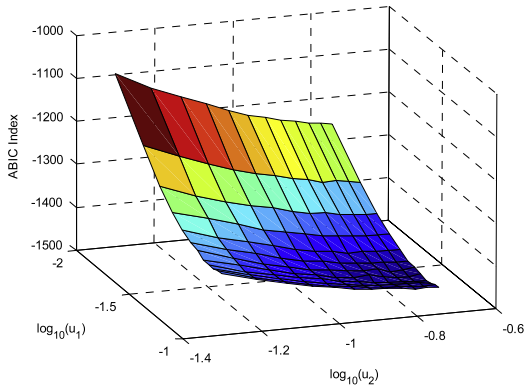

Fig. 14. ABIC criterion map — P35L120B5 test.

Application of the ABIC criterion for defining the optimum set of hyperparameters was tested and proved to enhance the overall accuracy of the predictions. Nonetheless, it still requires a considerable computational effort and its application does not seem appropriate from a practical point of view, at least when on-board predictions are sought to provide expedite operational information for the vessel's crew. In face of this problem, a different procedure was adopted for which the values of the hyperparameters were previously "calibrated" based on a set of numerical trials and kept fixed for each loading. Through this analysis it was possible to observe that the sensitivity to these values decreases with the magnitude of the motions, as could be anticipated. Therefore, errors resulting from a bad selection of these values tend to become more significant as the vessel loading increases.

Results have shown that majority of wave conditions can be accurately inferred from the Bayesian method. Even for demanding situations involving mild seas (of relatively low amplitudes and periods), the errors were, in most cases, kept within reasonable limits.

The occurrence of an 180° mismatch in the predicted wave direction, previously mentioned by other authors as an occasional drawback, was not observed in any case. It was shown that particularities of the heave transfer functions indeed have an influence on the estimations, but eventual errors derived from the absence of vertical motions are confined to a quite narrow range of frequencies and they are not sufficient to cause significant distortion of the estimated statistical figures. Moreover, it was shown that this problem can be avoided with a correct selection of the hyperparameters, by imposing that the spectrum distribution in frequency is sufficiently smooth. Therefore, contrary to the opinion of Pascoal et al. [8], the characteristics of their RAOs do not disqualify large vessels as adequate sensors for motion-based estimations.

In summary, the whole set of experimental results reassures the feasibility of estimating directional wave spectra based on 1st order vessel motions. The only noteworthy limitation of the method is related to the range of wave frequencies that might be inferred, since the vessel behaves like a low-pass filter. Obviously, for accurate estimations, the vessel must have a reasonable response in face of the waves it wishes to estimate. Each vessel will have a distinct range of accurate predictions, depending on its size and inertial properties. Nevertheless, it is important to recall that many of the possible applications envisaged for on-board wave measurements are concerned precisely with the situations when the waves do induce significant vessel motions.

Conclusions derived from the wave basin tests seem to be easily extended to the real-scale problem. In this case, however, attention should be paid to the calculation of the transfer functions as they shall be influenced by the presence of moonpools and by the characteristics of the mooring system, for example. Such influences can be easily dealt with nowadays by combining the results of BEM codes, such as WAMIT®, with well-established time-domain simulators that deal with the coupled dynamics of moored systems. Also, in the case of basing the estimations on offshore units that operate with variable loading (such as the FPSOs), continuous information on the cargo has to be provided. Most offshore units have systems that rigorously check its loading from time to time, and this information may be used for the estimations. As a final step of the ongoing research project, a field campaign will be performed in the near future and shall bring valuable information to the discussion of full-scale applications.

Acknowledgements

Authors gratefully acknowledge Petrobras for supporting the research project conducted at the University of São Paulo and providing the funds that made this experimental campaign possible. First and second authors acknowledge CNPq, the Brazilian National Research Council, for their respective research-grants. Third author also thanks CNPq for granting his DSc scholarship.

P35L120B5 ABIC	Experimental	Bayesian	Errors
Hs (m)	1.49	1.52	1.9%
Tp (s)	11.40	9.67	-15.2%
Direction (°)	105.04	118.70	13.7°

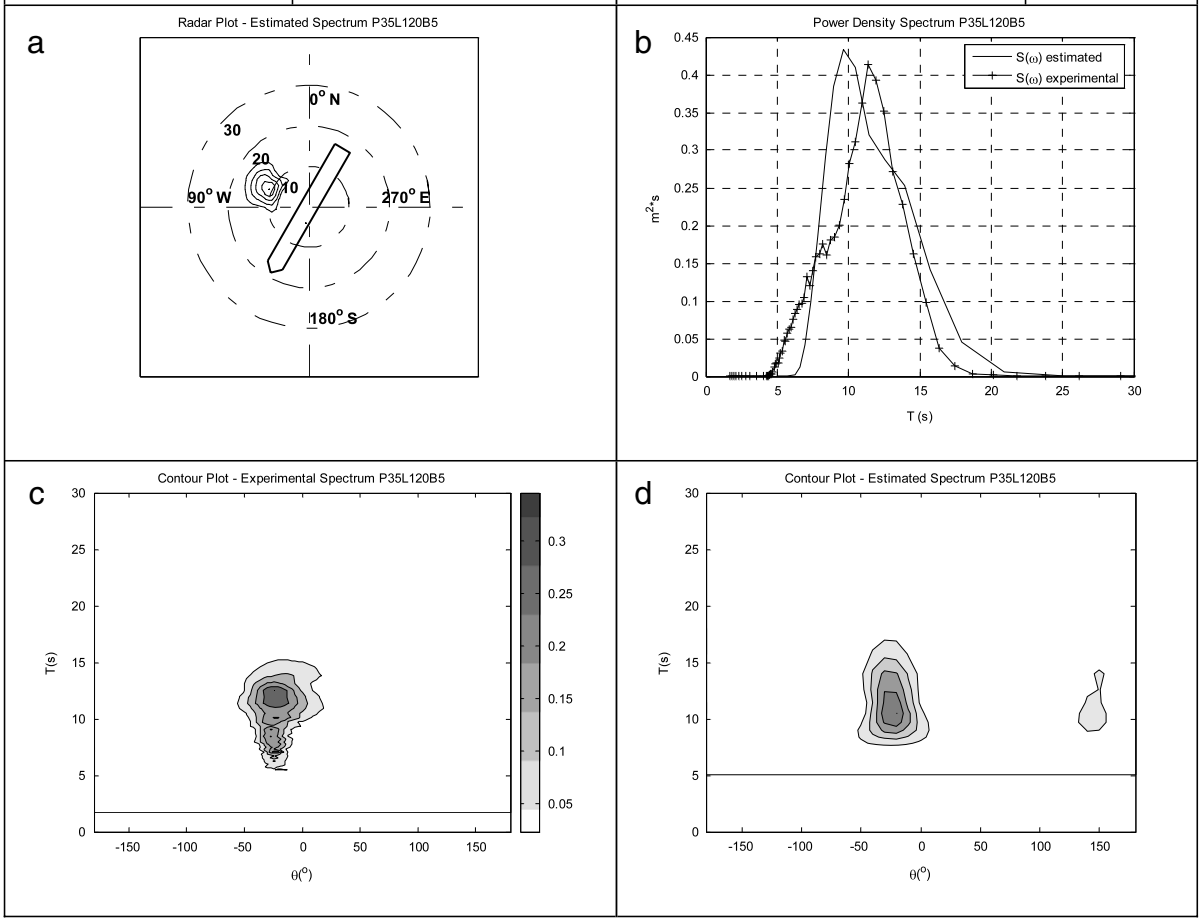

Fig. 15. Estimation results using ABIC criterion — P35L120B5 test.

References

[1] Hua J, Palmquist M. Wave estimation through ship motion measurement. Technical report, Naval Arch., Dept. of Vehicle Eng., Royal Institute of Technology; 1994.

[2] Tannuri EA, Sparano JV, Simos AN, Da Cruz JJ. Estimating directional wave spectrum based on stationary ship motion measurements. Applied Ocean Research 2004;25:243–61.

[3] Nielsen UD. Response-based estimation of sea state parameters — Influence of filtering. Ocean Engineering 2007;34:1797–810.

[4] Nielsen UD. Estimations of on-site directional wave spectra from measured ship responses. Marine Structures 2006;19:33–69.

[5] Iseki T, Ohtsu K. Bayesian estimation of directional wave spectra based on ship motions. Control Engineering Practice 2000;8:215–9.

[6] Akaike H. Likelihood and Bayes procedure. In: Bernardo JM, de Groot MH, Lindley DU, Smith AFM, editors. Bayesian statistics. Valencia: University Press; 1980. p. 143–66.

[7] Nielsen UD. Introducing two hyperparameters in Bayesian estimation of wave spectra. Probabilistic Engineering Mechanics 2008;23:84–94.

[8] Pascoal R, Guedes Soares C, Sorensen AJ. Ocean wave spectral estimation using vessel wave frequency motions. In: Proc. of the 24th int. conf. on offshore mech. and artic eng. OMAE2005, Haikidiki, Greece: ASME; 2005. p. 12–7. Paper OMAE2005-67584.

[9] Iseki T. Extended Bayesian estimation of directional wave spectra. In: Proc. of the 23rd int. conf. on offshore mech. and arctic eng., (OMAE2004). Vancouver (Canada): ASME; 2004. Paper OMAE2004-51609.

[10] Simos AN, Sparano JV, Tannuri EA, Matos VLF. Directional wave spectrum estimation based on a vessel 1st order motions: Field results. In: The 17th international offshore and polar engineering conference. 2007.

[11] Stansberg CT. On the Fourier series decomposition of directional wave spectra. In: Proc. of the 8th int. off and polar eng. conf. 1998, p. 227–33.

[12] Tannuri EA, Mello PC, Sales JS Jr., Simos AN, Matos VLF. Estimation of directional wave spectrum using a wave-probe array. In: Proc. of 3rd int. workshop on applied offshore hydrodynamics. 2007.

[13] WAMIT. Wave analysis program: Reference manual. WAMIT, Inc.; 2000.